

Chapter 11

Microfluidic Systems with Functional Patterned Surface for Biomedical Applications

Kin Fong Lei, I-Chi Lee and Tim C. Lei

11.1 Introduction

In the past decades, microfluidics system, also called “lab-on-chip (LOC),” “biochip,” or “micro-total-analysis-system (μ TAS),” has been rapidly developed, and a number of biomedical applications have been demonstrated using microfluidic technology [1–4]. It is a very exciting multidisciplinary topic of the combination of engineering and life science. One of the objectives of the development is to substitute the bioanalytical equipment performing in a conventional laboratory to an automated and miniaturized device operating in a remote environment. A total solution starting from sample pretreatment, sample/reagent manipulation, separation, reaction, detection, to analytical result display can be automatically conducted in a single compact device. Due to their miniaturization and automation, there are a number of advantages of using microfluidic systems such as less sample/reagent consumption, reduced risk of contamination, less cost per analysis, lower power consumption, faster analysis, enhanced sensitivity and specificity, and higher reliability.

The development of microfluidic technology began from micro-electromechanical system (MEMS) manufacturing infrastructure, which is silicon-based fabrication process. Beside the conventional surface microfabrication technique, high-aspect ratio fabrication processes were specifically developed for MEMS such

K. F. Lei (✉)

Graduate Institute of Medical Mechatronics, Chang Gung University,
259 Wen-Hwa 1st Road, Kwei-Shan, Tao-Yuan, Taiwan 333
e-mail: kflei@mail.cgu.edu.tw

Department of Mechanical Engineering, Chang Gung University, Kwei-Shan, Tao-Yuan, Taiwan

I.-C. Lee

Graduate Institute of Biochemical and Biomedical Engineering,
Chang Gung University, Kwei-Shan, Tao-Yuan, Taiwan

T. C. Lei

Department of Electrical Engineering, University of Colorado Denver, Denver, USA

© Springer International Publishing Switzerland 2015

J. Rodríguez-Hernández, A. L. Cortajarena (eds.), *Design of Polymeric Platforms for Selective Biorecognition*, DOI 10.1007/978-3-319-17061-9_11

as deep reactive ion etching (DRIE), LIGA, and substrate bonding techniques [5–7]. Based on the well-established silicon microfabrication process and extensive studies of silicon property, development of microfluidic technology has rapidly grown and silicon-based microfluidic systems have been demonstrated on various fluidic functions [8–11]. However, most of the biological activities are commonly represented by optical signals. Silicon substrate is not optically transparent and may be limited to be used in the biomedical applications. Hence, glass and polymer materials were introduced for the substrates of microfluidic systems. Polymer materials include polymethylmethacrylate (PMMA), polystyrene (PS), polycarbonate (PC), and polydimethylsiloxane (PDMS) and they are less expensive, flexible, optically transparent, and biocompatible. Some newly developed fabrication techniques were proposed such as soft lithography, hot embossing, injection molding, and low-temperature polymer bonding [12–16]. Currently, glass and polymer materials are the most widely used substrates for the development of microfluidic systems [17–19], and a lot of excellent demonstrations have been reported for diagnostic applications [1, 20]. These systems are much more automated and miniaturized and may achieve the objective of substitution of bioanalytical equipment performing in a conventional laboratory. But for the applications specifically aimed at rapid diagnostics, they are still not readily accessible to untrained personnel and are not appropriate for remote environment [21]. Most recently, paper has been proposed to be an alternative material used for the substrates of the microfluidic systems. It has the advantages of low cost, biocompatibility, disposability, and passive aqueous transportation and was suggested to be suitable for rapid diagnostics in remote environment [22]. The paper-based microfluidic systems can be realized by patterning sheets of paper into hydrophilic channels bounded by hydrophobic barriers based on the technologies of photolithography [23, 24], wax printing [25, 26], polydimethylsiloxane (PDMS) printing [27], and plasma treatment [28]. Based on these fabrication techniques, a number of biomedical applications have been demonstrated including colorimetric bio-assays [22, 29–30], electrochemical bio-assays [23, 31, 32], and paper-based enzyme-linked immunosorbent assay (ELISA) [33–36]. Conclusively, a broad spectrum of materials and fabrication techniques have been used and developed for the microfluidic systems. The technology is mature to design and fabricate automated and miniaturized devices for various applications.

A wide range of biomedical applications have been implemented to the microfluidic systems, such as DNA analysis [37–42], immunoassay [43–47], and cell analysis [48–52]. These demonstrations showed the power of microfluidic technology and its capability of performing complex analytical problems. In addition, in order to have more specific functions in microfluidic systems, surface modifications were introduced to improve the performance of the systems. The aim of this chapter focuses some of the recent developments of functional patterned surfaces in microfluidic systems. In-depth discussions of the surface modification technologies and their applications of fluid manipulation, suppression of biomolecule adsorption, control of cellular behavior, and biosensing are respectively included. The current excellent integration of microfluidic technology and surface chemistry suggests a solid foundation for the development of practical biomedical applications.

11.2 Modification of Surface Wetting Property

Surface wetting property can be modified to become hydrophobic or hydrophilic. Hydrophobic surfaces can be produced by coating hydrophobic non-polar molecules on top of them. With the hydrophobic coating, water on the surface exhibits a high contact angle θ , as illustrated in Fig. 11.1a. The determination of the contact angle is based on the result of the mechanical equilibrium of a droplet resting on a solid surface [53]. This is the action of three surface tensions: γ_{LG} at the interface of the liquid and gas; γ_{SL} at the interface of the solid and liquid; and γ_{SG} at the interface of the solid and gas. In contrast, hydrophilic surface is the surface modified by hydrophilic molecules which attract water. That is, water on hydrophilic surface exhibits a low contact angle, as illustrated in Fig. 11.1b. In general, if the water contact angle is larger than 90° , the solid surface is considered as hydrophobic, and if the water contact angle is smaller than 90° , the solid surface is considered to be hydrophilic. Surface wetting property can be modified by coating a layer of self-assembled monolayer (SAM). In the following, applications of fluid manipulation and suppression of bimolecular absorption through controlling the surface wetting property are discussed in this section.

11.2.1 SAM Coating

SAM of an organic molecule is a molecular assembly formed spontaneously on a surface. In some cases, SAM consists of head group, tail, and functional end group, as illustrated in Fig. 11.2. The head group has a strong affinity to the substrate and anchoring the molecule to the surface. Common head groups include thiols, silanes, and phosphonates. SAM can be created by first chemisorbing the molecules to the substrate with the head groups through vapor or lipid phase deposition. A slow reorganization of the tails of the molecules after the deposition forms the SAM coating. Finally, substrate surface is covered in a single monolayer. Depending on

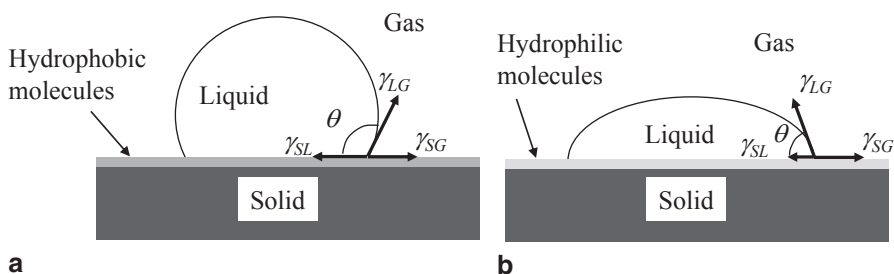
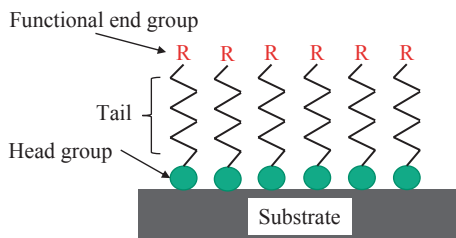


Fig. 11.1 Illustration of surface wetting property. **a** Water on hydrophobic surface. **b** Water on hydrophilic surface

Fig. 11.2 Representation of an SAM structure



the molecular property of the SAM, either hydrophobic or hydrophilic surface can therefore be created.

Silicon and glass surfaces consist of siloxane (Si-O-Si) bonds, which can rapidly acquire silanol (Si-OH) groups after contacting with water or atmospheric moisture. These -OH groups are polar and therefore make the surface hydrophilic [54]. Typically, a bare glass surface has a water contact angle of around 70–80°. To further enhance the hydrophilic property of the surface, SAM can be coated, and the water contact angle of the SAM-treated surface can be achieved to be as low as 40°. Example of the widely used hydrophilic molecule immobilized on glass substrate is 2-methoxy(polyethylenoxy)propyl trichlorosilane (PEG-silane). In contrast, octadecyltrichlorosilane (OTS) is the most commonly used hydrophobic molecule to change the substrate to be hydrophobic. The water contact angle of an OTS-treated surface is typically around 110°. A silicon or a glass surface can be dipped into an organic solvent dissolved with SAM molecules, such as hexadecane (HD) or dichloromethane. Illustration of the process is shown in Fig. 11.3. The trichlorosilane (HSiCl₃) group of the SAM molecules acts as the polar end of an amphiphilic molecule and attracts a layer of water to be bound to the silanol groups of the silicon or glass surface. Upon contact with water, the molecule is hydrolyzed with the elimination of HCl. The -OH groups of the molecules are then created hydrogen bonds with the silanol groups at the substrate surface with the elimination of H₂O. Finally, SAM can be coated on the entire substrate surface to modify the substrate surface wetting property.

PDMS is also a widely used material for the development of microfluidic systems. Original PDMS surface is hydrophobic and has a water contact angle of around 110°. To modify PDMS surface to be hydrophilic, plasma activation or SAM coat-

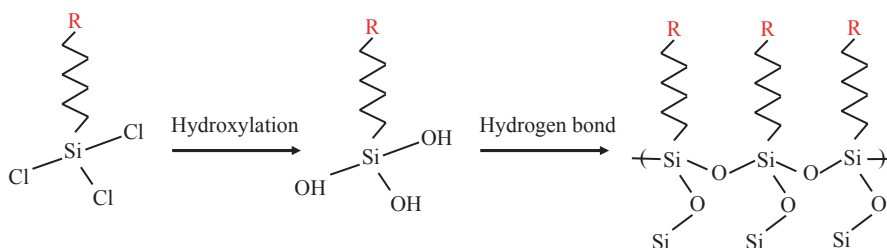


Fig. 11.3 Formation of SAM molecules on silicon or glass surface

ing can be used. In plasma activation, hydrogen atoms of PDMS are first removed from the polymer chain, and the activated surface reacts with the oxygen or moisture in the air, forming SiO_2 , Si-OH , or $\text{Si-CH}_2\text{OH}$ groups on the PDMS surface [55, 56]. These polar groups make the surface hydrophilic immediately after the plasma treatment. However, the surface regains its original hydrophobic character after several days. In order to stabilize the surface wetting property, incorporation of monomer molecules, e.g., poly(ethylene glycol) (PEG) and poly(oxyethylene) (POE), can modify the PDMS surface to be hydrophilic. These molecules have polar groups that increase dipole–dipole interactions. The PDMS surface finally has a water contact angle of around 40° . By coating the SAM, the surface wetting property of PDMS material can be modified.

11.2.2 Application Examples—Fluid Manipulation

Fluid manipulation in microfluidic systems can be realized by various fluid components such as micropumps [57, 58] and microvalves [59, 60]. To generate pumping and valving functions, most of these components were composed of moving parts and involved complicated fabrication process. An alternative method was proposed to modify the surface wetting property to induce passive pumping and valving functions. By special arrangement of hydrophilic and hydrophobic surfaces in the microfluidic systems, passive fluid manipulation can be realized without moving parts. To pattern hydrophobic and hydrophilic SAM in microfluidic systems, multi-stream laminar flow and UV photolithography were respectively proposed [61–63]. The former one was to pattern the surface inside channel networks by combining multistream liquid laminar flow and SAM chemistry. Pressure-sensitive microfluidic gates were demonstrated, and hydrophobic molecules of OTS and heptadecafluoro-1,1,2,2-tetrahydrodecyltrichlorosilane (HFTS) were used to coat on glass surface [62]. Three solutions of HD, OTS in HD, and HFTS in HD were pumped into the channels and maintained under laminar flow for a predetermined period of time, as illustrated in Fig. 11.4a. Hence, SAMs formed on the top and bottom substrates of the channels simultaneously in the areas where OTS and HFTS solutions flowed through, while other areas remained hydrophilic. Once the surface was patterned, aqueous dye solution was pumped along the hydrophilic pathway at three different pressures of spontaneous flow, 26 mmH_2O , and 39 mmH_2O . As shown in Fig. 11.4b–d, solution was confined to the hydrophilic pathway under spontaneous flow condition and flowed into the hydrophobic regions when pressures exceeded critical values.

Alternatively, patterning the surface by UV photolithography combined with photocleavable SMA of 2,2,3,3,4,4,5,5,6,6,7,7,8,8-pentadecafluoro-1-octyl 4-(11-trichlorosilyl-1-oxoundecyloxymethyl)-3-nitrobenzoate (F-SAM) was reported to generate hydrophilic and hydrophobic surface patterns for fabricating microfluidic gates [62]. Upon exposure to UV irradiation, the *o*-nitrobenzyl-oxygen bond in the F-SAM was cleaved and thus the carboxylic acid groups were exposed to the air interface, making the surface hydrophilic. Illustration of photodeprotection

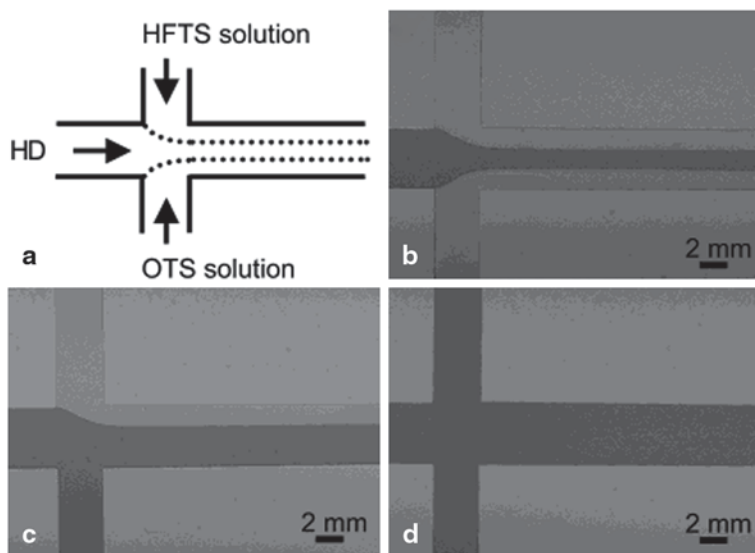


Fig. 11.4 **a** Schematic illustrations of multistream laminar flow of HD, a solution of OTS in HD, and a solution of HFTS in HD. **b-d** Optical micrograph of an aqueous dye solution flowing **b** along the hydrophilic pathway under spontaneous flow conditions, **c** into the OTS region under a pressure of 26 mmH₂O, and **d** into the HFTS region under a pressure of 39 mmH₂O. (Reprinted with permission from [62]. Copyright (2003) American Chemistry Society.)

of F-SAM upon exposure to UV irradiation is shown in Fig. 11.5a. The water contact angle on F-SAM-coated cover glass could be adjusted by the UV irradiation time, as shown in Fig. 11.5b. The contact angle decreased rapidly in the beginning but leveled off after 90 min. Thus, patterning different surface wetting properties inside microchannel was demonstrated by different irradiation times on the F-SAM-coated surface. As shown in Fig. 11.6a, regions A and B were irradiated for 120 and 60 min, respectively, resulting in the contact angles of 69° and 76°, respectively. Under spontaneous flow condition, water was confined in region A, as shown in Fig. 11.6b. Increasing water pressure led to water flowing into region B, as shown in Fig. 11.6c, d. As there was no physical wall on the sides of the liquid streams, liquid was referred to as being confined by virtual walls.

11.2.3 Application Examples—Suppression of Biomolecule Adsorption

Hydrophobic surfaces cause adsorption of significant amounts of protein from the surrounding biological environment, resulted in microbial adhesion and biofilm formation. In some cases, the adsorption of nonspecific proteins leads to failure of the

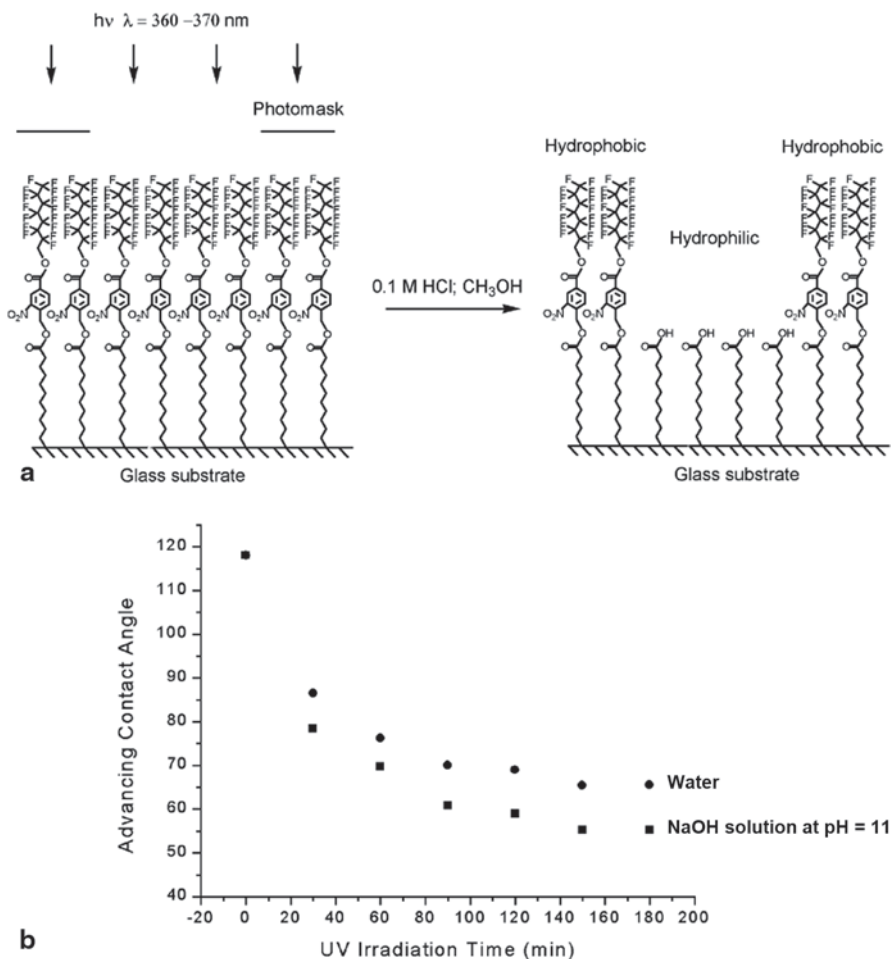


Fig. 11.5 **a** Photodeprotection of F-SAM upon exposure to UV irradiation. **b** Effect of UV irradiation time on the surface wettability of F-SAM. (Reprinted with permission from [62]. Copyright (2003) American Chemistry Society.)

device [64, 65]. Therefore, it is desirable to modify surfaces of the devices to reduce absorption of proteins and adhesion of cells [66–69]. These were demonstrated by PEG-grafted PDMS surfaces [68]. The monomer of polyethylene glycol diacrylate (PEGDA) was used, and the micropatterned PEGDA-grafted PDMS surface was prepared by photo-induced graft polymerization. After an application of PEGDA on the surface, UV light was irradiated through a photomask with an array of black squares to obtain a completely grafted surface. The PDMS surface was then rinsed and dried. Fluorescein isothiocyanate-labeled bovine albumin (FITC-BSA) and HepG2 cells were respectively added to the micropatterned PEGDA-grafted PDMS surfaces and were then incubated. Adsorption of FITC-BSA and HepG2 cells are

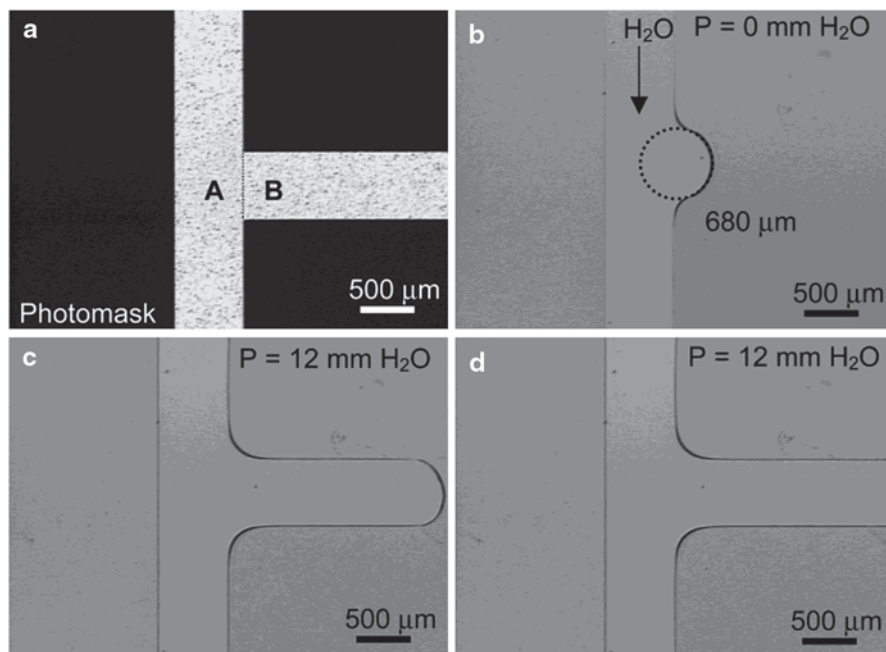


Fig. 11.6 **a** Optical micrograph of the photomask that was used in patterning surface free energies inside a microchannel. **b** Optical micrograph of a water stream under spontaneous flow condition. **c, d** Optical micrographs of water flow under a pressure of 12 mm H₂O recorded at different times. (Reprinted with permission from [62]. Copyright (2003) American Chemistry Society.)

respectively shown in Fig. 11.7 and Fig. 11.8. The green fluorescence intensity was proportional to the amount of the adsorbed BSA and suggested that the untreated PDMS area adsorbed more proteins than the PEGDA-grafted area. The HepG2 cells were not observed to attach to the PEG-covered area. These results indicated that the PEGDA-grafted layer prevents nonspecific protein adsorption and cell adhesion on PDMS.

A more specific biomedical application requiring suppression of biomolecule adsorption is electrophoretic separations of biological compounds. PDMS microfluidic devices are hampered with unwanted adsorption of biomolecules. Covalent coating of POE molecules of varying chain lengths as well as physical adsorption of triblock-copolymers of Pluronic® F108 and L101 on PDMS surface were performed to compare the electroosmotic mobilities of microchannels [69]. Results revealed that all of the above surface coatings led to reductions of electroosmotic flow. However, molecules with smaller POE tails, such as Si-POE₍₈₎ and L101, were the least effective. Molecules with longer POE tails (POE units > 70) are more effective but risk a consequence of lower electroosmotic velocity per unit field strength. Therefore, tailoring POE length may be a good parameter to control electroosmotic velocity in PDMS microchannels.

Fig. 11.7 FITC-BSA adsorption onto the micropatterned PEGDA-grafted PDMS. (Reprinted with permission from [68]. Copyright (2008) Elsevier.)

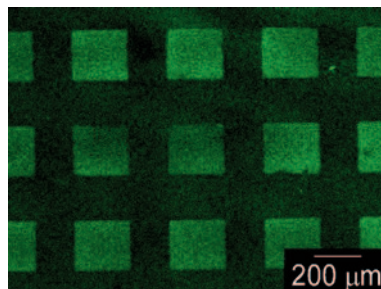
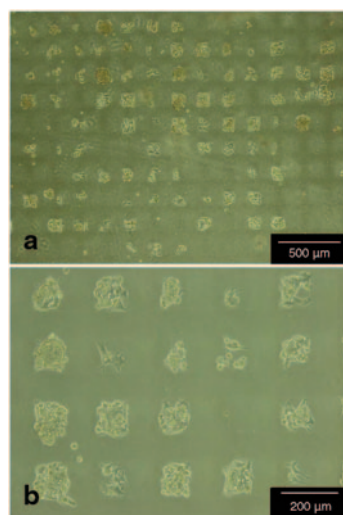


Fig. 11.8 Optical micrographs of HepG2 cells cultured on the micropatterned PEGDA-grafted PDMS observed through **a** a 4× objective lens and **b** a 10× objective lens. (Reprinted with permission from [68]. Copyright (2008) Elsevier.)



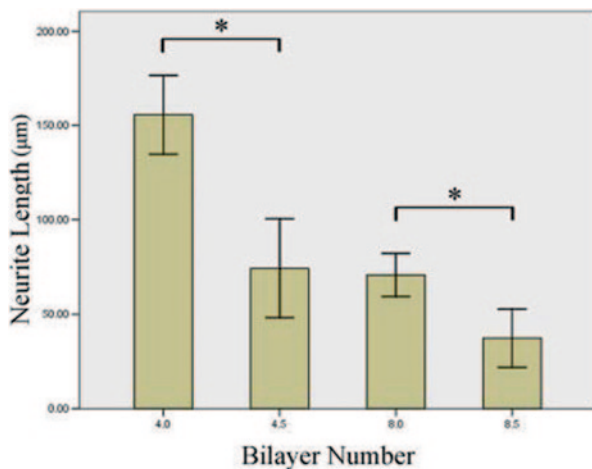
11.3 Creation of Cyto-compatible Surfaces

To promote the cell adhesion on the substrate surface, protein and peptide molecules were used as coating materials, such as fibronectin protein [70] and Arg-Gly-Asp (RGD) peptide [71]. Better cell attachment was demonstrated on these immobilized surfaces, but the protein and peptide immobilization processes involve complicated protocol which may lead to uncontrollable surface absorption. Therefore, development of new coating techniques was being pursued to improve cyto-compatibility using extracellular matrix (ECM) components and microstructures. In this section, the use of polyelectrolyte multilayer (PEM) film on solid surfaces to control cellular behaviors is being discussed.

11.3.1 PEM Film Coating

Coating a PEM film on a solid surface relies on nonstoichiometric electrostatic interactions and cationic and anionic polyelectrolyte layers are absorbed to the surface

Fig. 11.9 The neurite length of neurons was compared with (HA/COL)_n films with different terminated out-layers using Student's *t* test in the group of close bilayer numbers. Error bars show standard deviation of the mean. **p* < 0.01. (Reprinted with permission from [75]. Copyright (2006) Wiley Periodicals, Inc.)



alternatively. Poly-L-lysine (PLL) is positively charged and is widely used for promoting cell adhesion to solid surfaces [72, 73]. Poly-L-glutamine acid (PLGA) is negatively charged and is known to be a biodegradable material [74]. Layer-by-layer assembly of PEM film has been demonstrated for the improvement of cytocompatibility and the control of cellular behavior [75–80]. This method provides adjustable film properties in terms of thickness, morphology, and internal molecular structure [81, 82].

11.3.2 Application Examples—Control of Cellular Behavior

Surface morphology of a hyaluronic acid (HA)-based PEM film (bilayer number <9) deposited on the amino-functionalized glass slides was investigated to have a nanoscale roughness ranging from 10 to 100 nm [75]. Primary hippocampal and cortical neural cells were cultured on the HA/Collagen type I (COL) PEM films for 5 days. The statistical results of neurite lengths of the neurons on different bilayer numbers of HA/COL films are shown in Fig. 11.9. The neurite lengths of the COL-terminated films were significantly longer than those of the HA-terminated films where they had a very close bilayer number. However, neurons grown on (HA/COL)_{4,5} and (HA/COL)₈ films had no significant difference in neurite lengths. It was pointed out that neurite outgrowth is not simply influenced by the last layer of the PE films but may also be related to the bilayer number and other surface properties.

Moreover, in vitro cultures of neural progenitor cells on PEM films built up by heparin and PLL were also studied to improve cell adhesion and subsequent cellular functions [79]. In this study, neuronal spreading (β III-Tubulin positive) was observed on both PLL positive controls and PLL-terminating PEM films (Fig. 11.10a–c). Neurites radially elongating and perpendicular side branching at the periphery of outgrowths were observed. For heparin terminating layers, while

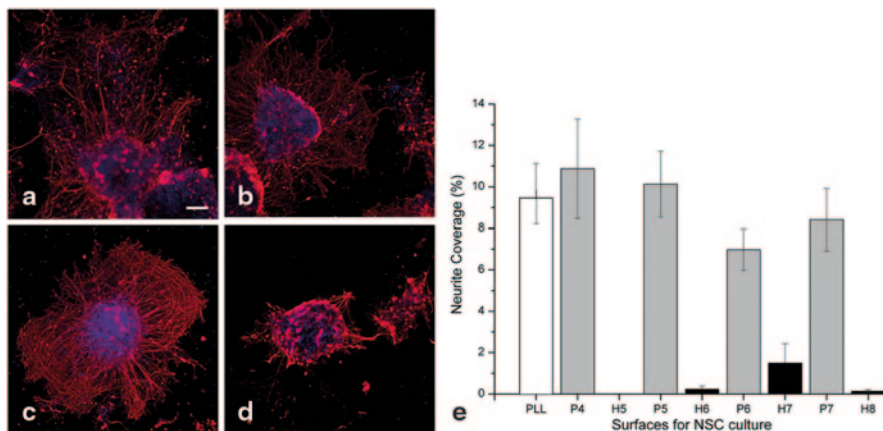


Fig. 11.10 **a** Cells cultured for 5 days on the PLL positive control, **b** P4, **c** P5, and **d** H6 PEM film surfaces. The cells were stained by β III-Tubulin (red) for neurons and DAPI (blue) for nuclei. Scale bar indicates 100 μ m in **a-d**. **e** Day 5 neurite coverage (from cell clusters) on the PLL positive control and the PEM films from P4 to H8. Error bars show standard deviation of the mean. (Reprinted with permission from [79]. Copyright (2011) American Vacuum Society.)

some cell colonies were seen to adhere, neurite elongations were relatively short and sparse (Fig. 11.10d). Based on the quantified neurite coverage shown in Fig. 11.10e, cell-substrate interactions were significantly improved on the PLL-terminating surfaces. In addition, brain-derived neurotrophic factor (BDNF) was adsorbed onto the PEM film surfaces. This combined chemical and biological effect was then characterized in terms of neurite length along with the full length/truncated isoform 1 tyrosine kinase receptor (TrkB-FL/TrkB-T1) and growth associated protein-43 mRNA levels. Here, the authors reported the differential effect of the adsorbed and soluble BDNF in different concentrations. The adsorbed BDNF promoted the neurite outgrowth and led to elevated, sustained TrkB mRNA levels.

11.4 Creation of Biological Specific Surfaces

Microfluidic systems were developed for various automated and miniaturized diagnostic applications [1]. In miniaturized environment, high surface-to-volume ratio can improve the sensitivity of biosensing when comparing to standard well format, but also magnify the effect of nonspecific binding of biomolecules. This is especially important in immunoassays that key reagents such as proteins and enzyme labels can adsorb to hydrophobic surfaces, seriously degrading the assay performance. Immunoassay is to measure the presence and the concentration of antibody or antigen in biological liquid. The detection method is generally based on protein binding reaction, which is a specific interaction between an antibody and its antigen. One of the challenges is to immobilize antibodies on the sensing

surface homogeneously and effectively to achieve accurate and sensitive detection. Creating an antibody-immobilized sensing surface to specifically capture a specific antigen is important for the development of the microfluidic biological sensing systems. Hence the concentration of the target antigen in the biological liquid can be measured correctly. Strategies that have been used to attach antibodies on the sensing surface include direct adsorption and covalent attachment to reactive functional groups on the substrate. Direct adsorption is commonly used on hydrophobic polymer surfaces but this technique may not be the most sensitive because of the conformational uncertainty. Therefore, covalent attachment is more preferable to have stable protein immobilization on the sensing surface.

11.4.1 Immobilization of Biomolecules

Surface modification by SAM on solid surfaces was employed to covalently immobilize protein on a surface. The functional end group of SAM can yield a number of active groups like $-OH$, $-NH_2$, $-COOH$, and $-COOR$ to attach proteins. Generally, proteins supply the following chemical functionalities on the side chains of their polypeptide backbone: $-SH$ (cysteine), $-NH_2$ (lysine, arginine), $-COOH$ (asparagine, glutamine), $-OH$ (serine), $Ph-OH$ (Ph =phenyl, tyrosine), and imidazole (histidine). In principle, all of them can be used during the direct chemical coupling reaction on specially prepared SAM surfaces. Several strategies on modifying silicon or glass surfaces were developed and are shown in Fig. 11.11: (1) glutaraldehyde (GA)-activated 3-aminopropyltriethoxysilane (APTES) (APTES-GA surface), (2) GA-activated physically adsorbed poly(ethyleneimine) (BPEI) (BPEI-GA surface), (3) GA-activated BPEI covalently attached to 3-glycidoxypolytrimethoxysilane (GOPS)-silanized surface (GOPS-BPEI-GA surface), (4) GA-activated physically adsorbed poly(ethyleneimine) (LPEI) (LPEI-GA surface), and (5) adsorption of antibodies on a physically adsorbed LPEI layer (LPEI surface) [83]. The detailed procedures of antibody immobilization based on different strategies are included below.

11.4.1.1 Immobilization of Antibodies onto APTES-GA Surface

Cleaned silicon or glass substrates are washed with sodium-dried toluene and then immersed in a solution of 10% APTES in dried toluene. Then the reaction mixture is refluxed overnight at room temperature. After removal of the solution, the substrates are rinsed several times with toluene and acetone and dried in an oven at $110^\circ C$ for 1 h. The amine groups of the APTES-silanized substrates are reacted with 2.5% v/v GA in buffer for 1 h at room temperature, followed by thorough rinsing with Milli-Q water in order to remove traces of GA to avoid cross-linking after adding antibodies. Antibody (1 mg/mL) in buffer is then added to the GA-activated surfaces to react overnight at $4^\circ C$ under gentle shaking. After 12 h, the residual aldehyde groups remained after antibody attachment are blocked with 10 mg/mL of L-lysine. The Schiff bases are reduced with 20 mg/mL $NaBH_3CN$ solution in buf-

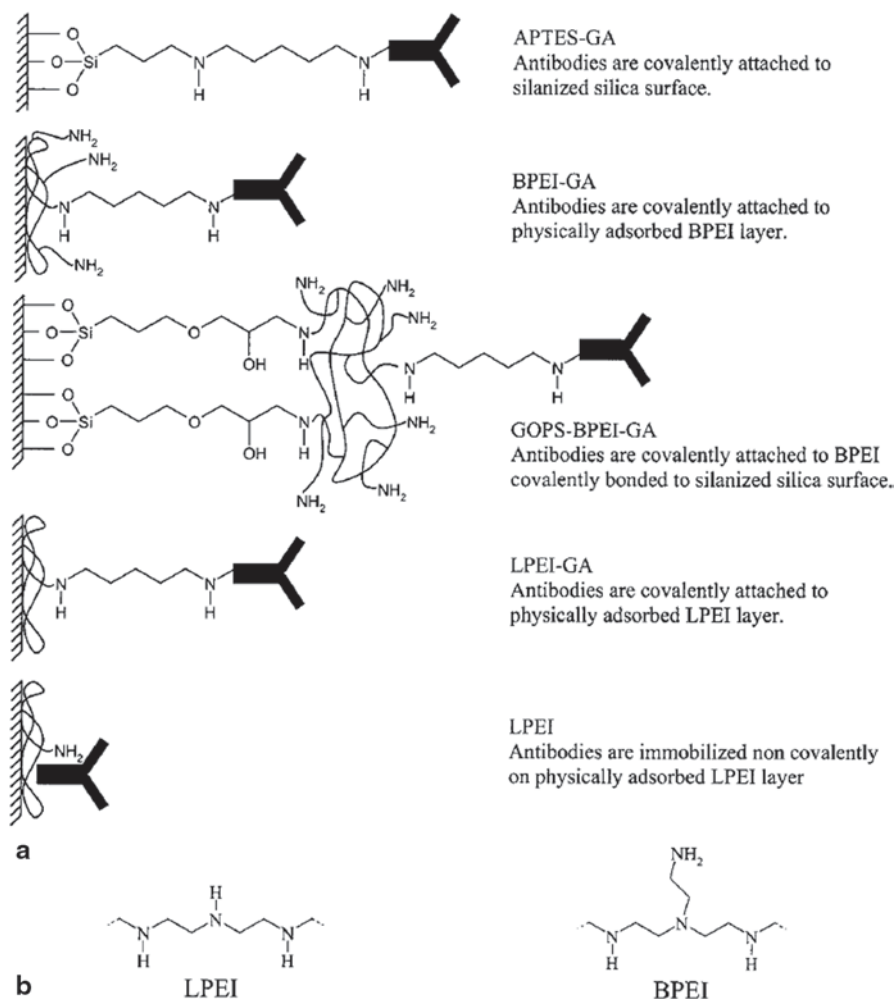


Fig. 11.11 **a** Structures of the modified surfaces for protein immobilization. **b** Chemical structures of LPEI and BPEI. (Reprinted with permission from [83]. Copyright (2002) American Chemistry Society.)

fer, and the reaction mixture is allowed to proceed for 1–2 h under stirring at room temperature. The substrates are then carefully washed and stored in 0.1 M Tris/HCl buffer at 4 °C until use.

11.4.1.2 Immobilization of Antibodies on BPEI-GA Surface

Cleaned substrates are immersed in 0.5% v/v solution of BPEI in buffer and kept under stirring at room temperature overnight and then thoroughly washed with buf-

fer. To incorporate active aldehyde groups, the substrates are reacted with 2.5% v/v GA in buffer for 2 h at room temperature under stirring. After careful washing with Milli-Q water and buffer, the aldehyde-functionalized surfaces are reacted with antibody solution overnight at 4 °C. Then the residual aldehyde groups on the surfaces are blocked and the Schiff bases reduced as described in Sect. 4.1.1.

11.4.1.3 Immobilization of Antibodies on GOPS-BPEI-GA Surface

The cleaned substrates are reacted with GOPS in dry toluene, containing 2% v/v GOPS and 0.2% triethylamine at room temperature. After 1 h, the GOPS-coated surfaces are rinsed with toluene, then with acetone, and then dried in an oven at 110 °C for 1 h. A solution of 0.5% v/v BPEI in succinate buffer is added, and the reaction mixture is gently shaken for 5 h at room temperature. After careful washing with Milli-Q water, the surfaces are treated with 2.5% v/v GA in buffer. After 2 h, the surfaces are rinsed and then immersed in antibody solution. The reaction is allowed to proceed overnight at 4 °C, after which the surfaces are blocked and reduced as described in Sect. 4.1.1.

11.4.1.4 Immobilization of Antibodies on LPEI-GA Surface

The cleaned substrates are immersed in 0.5% v/v solution of LPEI in buffer and kept under stirring at room temperature overnight and then thoroughly washed with buffer. The GA activation and antibody attachment steps are carried out as described in Sect. 4.1.1.

11.4.1.5 Adsorption of Antibodies on LPEI Surface

The cleaned substrates are immersed in 0.5% v/v solution of LPEI in buffer and kept under stirring at room temperature overnight. The surfaces are then carefully washed with Milli-Q water, immersed in solution of antibodies in buffer, and allowed to proceed overnight at 4 °C.

11.4.2 Application Examples—Biosensing

A miniaturized mosaic immunoassay was proposed based on patterning lines of antigens onto a surface by means of a microfluidic network [84]. Illustration of the strategy is shown in Fig. 11.12. The microfluidic network immobilized a series of antigens as narrow stripes on a planar substrate. After a blocking step, the antigens in each line could be recognized by specific analytes from a sample solution also guided over the substrate with a second microfluidic network. The resulting binding pattern could then be readily evaluated when analytes were tagged or developed by binding

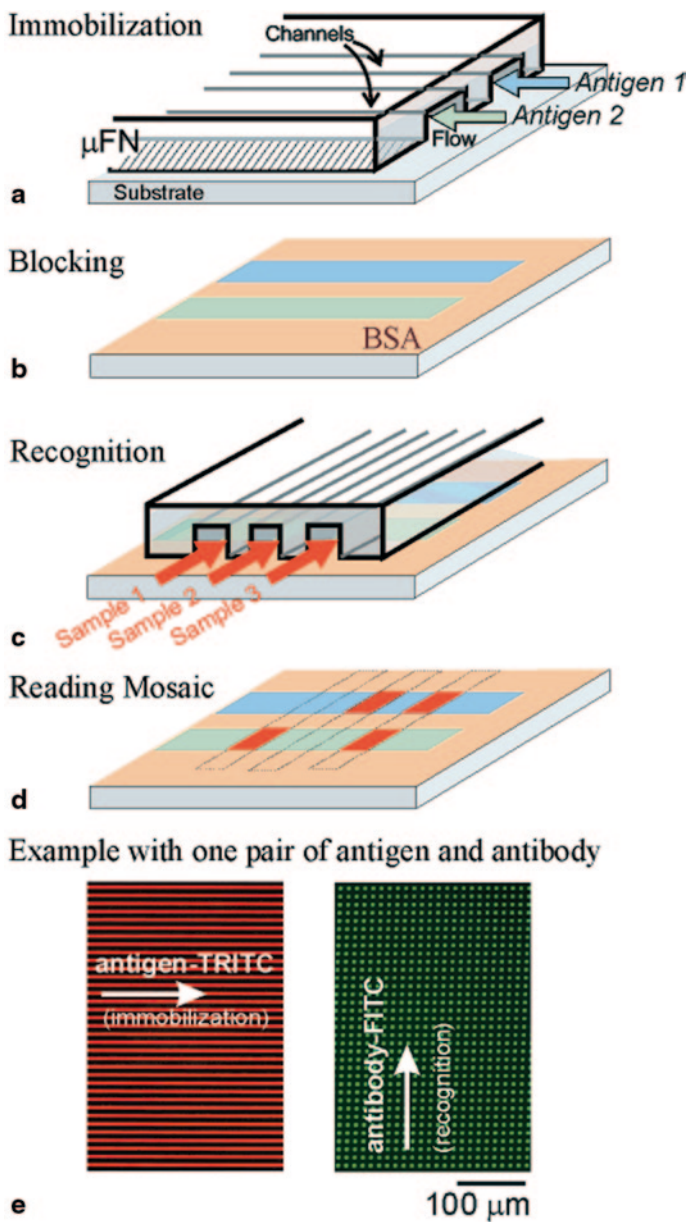


Fig. 11.12 Strategy for performing a micromosaic immunoassay on a surface with microfluidic network cross-delivery of a series of antigens and one of antibodies. **a** A microfluidic network patterns different antigen molecules along single lines on a substrates. **b** The area of the substrate left unpatterned during (a), it is blocked to prevent nonspecific binding of proteins in subsequent steps. **c** Antibodies flowing through the channels of a second microfluidic network locally bind to the patterned antigens. **d** Reading the binding mosaic reveals the amount of antibodies present in the samples. **e** A mosaic can be read using a fluorescence microscope. (Reprinted with permission from [84]. Copyright (2001) American Chemistry Society.)

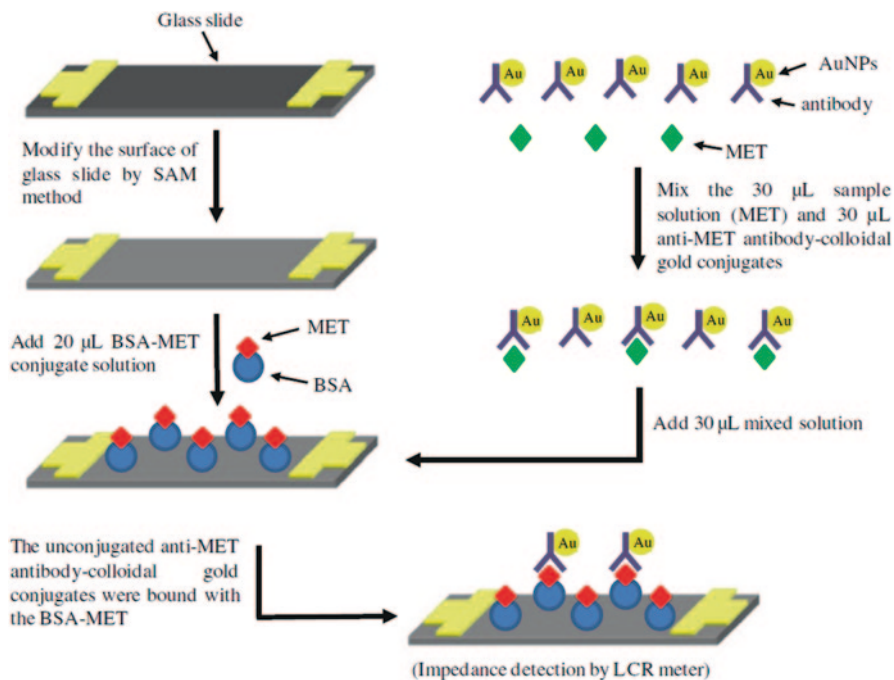


Fig. 11.13 Principle of the competitive immunoassay method for impedance detection of MET concentration. (Reprinted with permission from [86]. Copyright (2012) Springer.)

a fluorescent- or enzyme-conjugated antibody to the analyte. A mosaic of binding events can readily be measured in one screening using fluorescence. Similarly, large-scale protein microarray was also reported, and surface modification of the biological specific surfaces is one of the key challenges for such development [85].

The abovementioned example was to immobilize antibodies on the planar substrate, and the antigen-antibody interaction was indicated by fluorescent signal. The technique of protein immobilization is also important for specific and sensitive electrical immunoassay measurement. Electrical detection of protein concentration was developed based on the resistance measurement across a pair of indium tin oxide-interdigitated electrodes [44]. Antibody was first immobilized on the electrode surface and gold nanoparticles were then applied to indicate the concentration of the immobilized antibodies. Similar development was reported for methamphetamine (MET) detection [86]. Competitive immunoassay method was used in this study and illustrated in Fig. 11.13. The electrode on SAM modified glass slide was immobilized with bovine serum albumin (BSA)-MET conjugates. After sample solution of MET in urine was mixed with anti-MET antibody-colloidal gold conjugates for 1 min, the mixed solution was applied to the electrode surface, and the residual anti-MET antibody-colloidal gold conjugates were bound with BSA-MET conjugates. Consequently, the impedance across the electrode was measured and represented the concentration of the MET.

11.5 Concluding Remarks

Functional patterned surfaces provide a simple approach for selective biorecognition. This chapter reviewed the most commonly used surface modification technologies and their applications of fluid manipulation, suppression of biomolecule adsorption, control of cellular behavior, and biosensing in microfluidic systems. We anticipate that as these manufacturing and surface chemical techniques mature, microfluidic devices will be more widely used for many biomedical screening and diagnostics in the near future.

References

1. K.F. Lei, Microfluidic systems for diagnostic applications: A review. *JALA* 2012, 17, 330–347.
2. K.F. Lei, Review on impedance detection of cellular responses in micro/nano environment. *Micromachines* 2014, 5, 1–12.
3. H. Andersson, A. van den Berg, Microfluidic devices for cellomics: A review. *Sens Actuators B* 2003, 92, 315–325.
4. C. Zhang, J. Xu, W. Ma, W. Zheng, PCR Microfluidic devices for DNA amplification. *Biotech. Advances* 2006, 24, 243–284.
5. P. Pal, K. Sato, Various shapes of silicon freestanding microfluidic channels and microstructures in one-step lithography. *J. Micromech. Microeng.* 2009, 19, 055003–055013.
6. F. Marty, L. Rousseau, B. Saadany, B. Mercier, O. Francais, Y. Mita, T. Bourouina, Advanced etching of silicon based on deep reactive ion etching for silicon high aspect ratio microstructures and three-dimensional micro- and nanostructures. *Microelectron. J.* 2005, 36(7), 673–677.
7. M. Esashi, A. Nakano, S. Shoji, H. Hebiguchi, Low-temperature silicon-to-silicon anodic bonding with intermediate low melting point glan. *Sens. Actuators A* 1990, 23, 931–934.
8. P. Gravesen, J. Branebjerg, O.S. Jensen, Microfluidics-a review. *J. Micromech. Microeng.* 1993, 3, 168–182.
9. A. Luque, J.M. Quero, C. Hibert, P. Fluckiger, A.M. Ganan-Calvo, Integrable silicon microfluidic valve with pneumatic action. *Sens. Actuators A* 2005, 118(1), 144–151.
10. Y. Li, T. Pfohl, J.H. Kim, M. Yasa, Z. Wen, M.W. Kim, C.R. Safinya, Selective surface modification in silicon microfluidic channel for micromanipulation of biological macromolecules. *Biomed. Microdevices* 2001, 3(3), 239–244.
11. N.R. Harris, M. Hill, S. Beeby, Y. Shen, N.M. White, J.J. Hawkes, W.T. Coakley, A silicon microfluidic ultrasonic separator. *Sens. Actuators B* 2003, 95, 425–434.
12. Y. Xia, G.M. Whitesides, Soft lithography. *Annu. Rev. Mater. Sci.* 1998, 28, 153–184.
13. H. Becker, U. Heim, Hot embossing as a method for the fabrication of polymer high aspect ratio structures. *Sens. Actuators A* 2000, 83(1–3), 130–135.
14. U.M. Attia, S. Marson, J.R. Alcock, Micro-injection moulding of polymer microfluidic devices. *Microfluid. Nanofluid.* 2009, 7, 1–28.
15. K.F. Lei, S. Ahsan, N. Budraa, W.J. Li, J.D. Mai, Microwave bonding of polymer-based substrates for potential encapsulated micro/nano device fabrication. *Sens. Actuators A* 2004, 114(2–3), 340–346.
16. C.W. Tsao, D.L. DeVoe, Bonding of thermoplastic polymer microfluidics. *Microfluid. Nanofluid.* 2009, 6, 1–16.
17. M.A. Unger, H.P. Chou, T. Thorsen, A. Scherer, S.R. Quake, Monolithic microfabricated valves and pumps by multilayer soft lithography. *Science* 2000, 288, 113–116.

18. H. Becker, L.E. Locascio, Polymer microfluidic devices. *Talanta* 2002, 56(2), 267–287.
19. B. Kuswandi, Nuriman, J. Huskens, W. Verboom, Optical sensing systems for microfluidic devices: A review. *Anal. Chim. Acta* 2007, 601(2), 141–155.
20. S.E. McCalla, A. Tripathi, Microfluidic reactors for diagnostics applications. *Annu. Rev. Biomed. Eng.* 2011, 13, 321–343.
21. G.M. Whitesides, The origins and the future of microfluidics. *Nature* 2006, 442, 368–373.
22. A.W. Martinez, S.T. Phillips, G.M. Whitesides, Diagnostics for the developing world: microfluidic paper-based analytical devices. *Anal. Chem.* 2010, 82(1), 3–10.
23. W. Dungchai, O. Chailapakul, C.S. Henry, Electrochemical detection for paper-based microfluidics. *Anal. Chem.* 2009, 81, 5821–5826.
24. A.W. Martinez, S.T. Phillips, B.J. Wiley, M. Gupta, G.M. Whitesides, FLASH: A rapid method for prototyping paper-based microfluidic devices. *Lab Chip* 2008, 8, 2146–2150.
25. E. Carrilho, A.W. Martinez, G.M. Whitesides, Understanding wax printing: A simple micro-patterning process for paper-based microfluidics. *Anal. Chem.* 2009, 81, 7091–7095.
26. Y. Lu, W. Shi, L. Jiang, J. Qin, B. Lin, Rapid prototyping of paper-based microfluidics with wax for low-cost, portable bioassay. *Electrophoresis* 2009, 30, 1497–1500.
27. D.A. Bruzewicz, M. Reches, G.M. Whitesides, Low-cost printing of poly(dimethylsiloxane) barriers to define microchannels in paper. *Anal. Chem.* 2008, 80, 3387–3392.
28. X. Li, J. Tian, T. Nguyen, W. Shen, Paper-based microfluidic devices by plasma treatment. *Anal. Chem.* 2006, 80, 9131–9134.
29. W. Zhao, M.M. All, S.D. Aguirre, M.A. Brook, Y. Li, Paper-based bioassays using gold nanoparticle colorimetric probes. *Anal. Chem.* 2008, 80, 8431–8437.
30. A.K. Ellerbee, S.T. Phillips, A.C. Siegel, K.A. Mlrica, A.W. Martinez, et al., Quantifying colorimetric assays in paper-based microfluidic devices by measuring the transmission of light through paper. *Anal. Chem.* 2009, 81, 8447–8452.
31. D. Zang, L. Ge, M. Yan, X. Song, J. Yu, Electrochemical immunoassay on a 3D microfluidic paper-based device. *Chem. Commun.* 2012, 48, 4683–4685.
32. Z. Nie, C.A. Nijhuis, J. Gong, X. Chen, A. Kumachev, et al., Electrochemical sensing in paper-based microfluidic devices. *Lab Chip* 2009, 10, 477–483.
33. C.M. Cheng, A.W. Martinez, J. Gong, C.R. Mace, S.T. Phillips, et al., Paper-based ELISA. *Angew. Chem. Int. Ed.* 2010, 49, 4771–4774.
34. R.C. Murdock, L. Shen, D.K. Griffin, N. Kelley-Loughnane, I. Papautsky, et al., Optimization of a paper-based ELISA for a human performance biomarker. *Anal. Chem.* 2013, 85, 11634–11642.
35. H.K. Wang, C.H. Tsai, K.H. Chen, C.T. Tang, J.S. Leou, et al., Cellulose-based diagnostic devices for diagnosing serotype-2 dengue fever in human serum. *Adv. Healthcare Mater.* 2013, 3(2), 187–196.
36. S. Wang, L. Ge, X. Song, J. Yu, S. Ge, et al., Paper-based chemiluminescence ELISA: lab-on-paper based on chitosan modified paper device and wax-screen-printing. *Biosens. Bioelectron.* 2012, 31, 212–218.
37. D. Erickson, X. Liu, U. Krull, D. Li, Electrokinetically Controlled DNA hybridization microfluidic chip enabling rapid target analysis. *Anal. Chem.* 2004, 76, 7269–7277.
38. G.B. Lee, S.H. Chen, G.R. Huang, W.C. Sung, Y.H. Lin, Microfabricated plastic chips by hot embossing methods and their applications for DNA separation and detection. *Sens. Actuators B* 2001, 75(1–2), 142–148.
39. L. Wang, P.C.H. Li, Microfluidic DNA microarray analysis: A review. *Anal. Chim. Acta* 2011, 687, 12–27.
40. X. Weng, H. Jiang, D. Li, Microfluidic DNA hybridization assays. *Microfluid. Nanofluid.* 2011, 11, 367–383.
41. K.F. Lei, H. Cheng, K.Y. Choy, L.M.C. Chow, Electrokinetic DNA concentration in micro systems. *Sens. Actuators A* 2009, 156, 381–387.
42. Y. He, M. Tsutsui, C. Fan, M. Taniguchi, T. Kawai, Gate manipulation of DNA capture into nanopores. *ACS Nano* 2011, 5, 8391–8397.
43. A.H. Diercks, A. Ozinsky, C.L. Hansen, J.M. Spotts, D.J. Rodriguez, A. Aderem, A microfluidic device for multiplexed protein detection in nano-liter volumes. *Anal. Biochem.* 2009, 386, 30–35.

44. K.F. Lei, Quantitative electrical detection of immobilized protein using gold nanoparticles and gold enhancement on a biochip. *Meas. Sci. Technol.* 2011, 22, 105802.
45. M. Hervas, M.A. Lopez, A. Escarpa, Electrochemical immunosensing on board microfluidic chip platforms. *TrAC Trends Anal. Chem.* 2012, 31, 109–128.
46. A.H.C. Ng, U. Uddayasankar, A.R. Wheeler, Immunoassays in microfluidic systems. *Anal. Bioanal. Chem.* 2010, 397, 991–1007.
47. A. Bhattacharyya, C.M. Klapperich, Design and testing of a disposable microfluidic chemiluminescent immunoassay for disease biomarkers in human serum samples. *Biomed. Microdevices* 2007, 9, 245–251.
48. F.T.G. van den Brink, E. Gool, J.P. Frimat, J. Borner, A. van den Berg, S. Le Gac, Parallel single-cell analysis microfluidic platform. *Electrophoresis* 2011, 32, 3094–3100.
49. R.N. Zare, S. Kim, Microfluidic platforms for single-cell analysis. *Annu. Rev. Biomed. Eng.* 2010, 12, 187–201.
50. M.H. Wu, S.B. Huang, G.B. Lee, Microfluidic cell culture systems for drug research. *Lab Chip* 2010, 10, 939–956.
51. K.F. Lei, P.H.M. Leung, Microelectrode array biosensor for the detection of *Legionella pneumophila*. *Microelectron. Eng.* 2012, 91, 174–177.
52. K.F. Lei, M.H. Wu, C.W. Hsu, Y.D. Chen, Real-time and non-invasive impedimetric monitoring of cell proliferation and chemosensitivity in a perfusion 3D cell culture microfluidic chip. *Bioelectron.* 2014, 51, 16–21.
53. A.W. Adamson. *Physical Chemistry of Surface*, Wiley, New York, 1990.
54. R.K. Iler. *The Chemistry of Silica*, Wiley, New York, 1979.
55. E.M. Liston, L. Martin, M.R. Wertheimer, Plasma surface modification of polymers for improved adhesion: a critical review. *J Adhesion Sci. Tech.* 1993, 7(10), 1091–1127.
56. C. Oehr, Plasma surface modification of polymers for biomedical use. *Nucl. Instrum. Meth. Phys. Res. B* 2003, 208, 40–47.
57. L.S. Jang, W.H. Kan, Peristaltic piezoelectric micropump system for biomedical applications. *Biomed. Microdevices* 2007, 9, 619–626.
58. F. Amirouche, Y. Zhou, T. Johnson, Current micropump technologies and their biomedical applications. *Microsyst. Tech.* 2009, 15, 647–666.
59. S. Zeng, B. Li, X. Su, J. Qin, B. Lin, Microvalve-actuated precise control of individual droplets in microfluidic devices. *Lab Chip* 2009, 9, 1340–1343.
60. K.W. Oh, C.H. Ahn, A review of microvalves. *J Micromech. Microeng.* 2006, 16, R13–R39.
61. B. Zhao, J.S. Moore, D.J. Beebe, Surface-directed liquid flow inside microchannels. *Science* 2001, 291, 1023–1026.
62. B. Zhao, J.S. Moore, D.J. Beebe, Pressure-sensitive microfluidic gates fabricated by patterning surface free energies inside microchannels. *Langmuir* 2003, 19, 1873–1879.
63. B. Zhao, J.S. Moore, D.J. Beebe, Principles of surface-directed liquid flow in microfluidic channels. *Anal. Chem.* 2002, 74(16), 4259–4268.
64. H. Chen, M.A. Brook, H. Sheardown, Silicon elastomers for reduced protein adsorption. *Biomaterials* 2004, 25, 2273–2282.
65. F. Abbasi, H. Mirzadeh, Adhesion between modified and unmodified poly(dimethylsiloxane) layers for a biomedical application. *Int. J. Adhes. Adhes.* 2004, 24, 247–257.
66. H. Makambe, J.H. Kim, K. Lim, N. Park, J.H. Hahn, Surface modification of poly(dimethyl siloxane) microchannels. *Electrophoresis* 2003, 24, 3607–3619.
67. S. Pinto, P. Alves, C.M. Matos, A.C. Santos, L.R. Rodrigues, J.A. Texeira, M.H. Gil, Poly(dimethyl siloxane) surface modification by low pressure plasma to improve its characteristics towards biomedical applications. *Colloid Surface B* 2010, 81, 20–26.
68. S. Sugiura, J. Edahiro, K. Sumaru, T. Kanamori, Surface modification of poly dimethylsiloxane with photo-grafted poly(ethylene glycol) for micropatterned protein adsorption and cell adhesion. *Colloids Surface B* 2008, 63, 301–305.
69. W. Hellmich, J. Regtmeier, T.T. Duong, R. Ros, D. Anselmetti, A. Ros, Poly(oxyethylene) based surface coatings for poly(dimethylsiloxane) microchannels. *Langmuir* 2005, 21, 7551–7557.

70. Vassanelli, S.; Fromherz, P. Transistor probes local potassium conductances in the adhesion region of cultured rat hippocampal neurons. *J. Neurosci.* 1999, 19, 6767–6773.
71. Davis, D. H.; Giannoulis, C. S.; Johnson, R. W.; Desai, T. A. Immobilization of RGD to < 111 > silicon surfaces for enhanced cell adhesion and proliferation. *Biomaterials* 2002, 23, 4019–4027.
72. V. Gribova, C. Gauthier-Rouviere, C. Albiges-Rizo, R. Auzely-Velty, C. Picart. Effect of RGD functionalization and stiffness modulation of polyelectrolyte multilayer films on muscle cell differentiation. *Acta Biomaterialia*. 2013, 9, 6468–6480.
73. L. Richert, P. Lavalle, D. Vautier, B. Senger, J.F. Stoltz, P. Schaaf, et al., Cell interactions with polyelectrolyte multilayer films. *Biomacromolecules* 2002, 3(6), 1170–1178.
74. B. Cao, S. Yan, K. Zhang, Z. Song, X. Chen, L. Cui, et al., Layer-by-layer assembled multilayer films of methoxypoly(ethylene glycol)-block-poly(alpha, l-glutamic acid) and chitosan with reduced cell adhesion. *Macromolecular Biosci.* 2011, 11(9), 1211–1217.
75. Z.R. Wu, J. Ma, B.F. Liu, Q.Y. Xu, F.Z. Cui, Layer-by-layer assembly of polyelectrolyte films improving cytocompatibility to neural cells. *J. Biomed. Mater. Res. A* 2007, 81 A, 355–362.
76. L. Richert, P. Lavalle, D. Vautier, B. Senger, J.F. Stoltz, et al., Cell interactions with polyelectrolyte multilayer films. *Biomacromolecules* 2002, 3, 1170–1178.
77. L. Richert, A. Youri, P. Schaaf, J.C. Voegel, C. Picart, pH dependent growth of poly(L-lysine)/poly(L-glutamic) acid multilayer films and their cell adhesion properties. *Surf. Sci.* 2004, 570, 13–29.
78. L. Richert, A. Schneider, D. Vautier, C. Vodououhe, N. Jessel, et al. Imaging cell interactions with native and crosslinked polyelectrolyte multilayers. *Cell Biochem. Biophys.* 2006, 44, 273–285.
79. K. Zhou, G.Z. Sun, C.C. Bernard, G.A. Thouas, D.R. Nisbet, et al., Optimizing interfacial features to regulate neural progenitor cells using polyelectrolyte multilayers and brain derived neurotrophic factor. *Biointerphases* 2011, 6, 187–199.
80. J. Almodóvar, S. Bacon, J. Gogolski, J.D. Kisiday, M.J. Kipper, Polysaccharide-based polyelectrolyte multilayer surface coatings can enhance mesenchymal stem cell response to adsorbed growth factors. *Biomacromolecules* 2010, 11, 2629–2639.
81. R. A McAloney, M. Sinyor, V. Dudnik, M.C. Goh, Atomic force microscopy studies of salt effects on polyelectrolyte multilayer film morphology. *Langmuir* 2001, 17, 6655–6663.
82. D. Yoo, S.S. Shiratori, M.F. Rubner, Controlling bilayer composition and surface wettability of sequentially adsorbed multilayers of weak polyelectrolytes. *Macromolecules* 1998, 31, 4309–4318.
83. J. Yakovleva, R. Davidsson, A. Lobanova, M. Bengtsson, S. Eremin, et al., Microfluidic enzyme immunoassay using silicon microchip with immobilized antibodies and chemiluminescence detection. *Anal. Chem.* 2002, 74, 2994–3004.
84. A. Bernard, B. Michel, E. Delamarche, Micromosaic Immunoassays. *Anal. Chem.* 2001, 73, 8–12.
85. M. Schaeferling, S. Schiller, H. Paul, M. Kruschina, P. Pavlickova, et al., Application of self-assembly techniques in the design of biocompatible protein microarray surfaces. *Electrophoresis* 2002, 23, 3097–3105.
86. C.H. Yeh, W.T. Wang, P.L. Shen, Y.C. Lin, A developed competitive immunoassay based on impedance measurements for methamphetamine detection. *Microfluid. Nanofluid.* 2012, 13, 319–329.